

Chapter 14

Smart Self-interference Suppression by Exploiting a Nonlinearity

Erwin Janssen, Hooman Habibi, Dusan Milosevic, Peter Baltus,
and Arthur van Roermund

Abstract A 1.8GHz RF amplifier implemented in 0.14 μ m CMOS with frequency-independent blocker suppression is presented. The blocker suppression functionality is obtained by the adaptation of a nonlinear input–output transfer according to the blocker amplitude. Since superposition does not apply to nonlinear transfer functions, the behavior of such a transfer for strong undesired signals is different from the behavior for weak desired signals, which is exploited here. In the presence of a 0 to +11 dBm RF blocker, a voltage gain for weak signals of respectively 7.6–9.4 dB and IIP3 >4 dBm are measured, while the blocker is suppressed by more than 35 dB. In case of no blocker present at the input, the circuit is set to amplifier mode providing 17 dB of voltage gain and an IIP3 of 6.6 dBm while consuming 3 mW. Application areas are coexistence in multi-radio devices and dealing with TX leakage in FDD systems.

14.1 Introduction

Modern handheld devices support a multitude of wireless standards, such as e.g. WLAN, Bluetooth, GSM, UMTS and GPS. In recent years, the number of standards has been increasing steadily. The coexistence of these multiple

E. Janssen (✉)

Department of Electrical Engineering, Mixed-signal Microelectronics, Eindhoven University of Technology, Eindhoven, Netherlands

NXP semiconductors, Eindhoven, Netherlands

e-mail: Erwin.Janssen@nxp.com

H. Habibi

Department of Electrical Engineering, Signal Processing Systems, Eindhoven University of Technology, Eindhoven, Netherlands

D. Milosevic • P. Baltus • A. van Roermund

Department of Electrical Engineering, Mixed-signal Microelectronics, Eindhoven University of Technology, Eindhoven, Netherlands

communication standards within a single device becomes therefore an increasingly important issue [1, 2].

Straightforward concepts to achieve reliable coexistence could either use filtering or time-sharing concepts. As filtering is often not sufficient and also not cost effective, present solutions usually apply time sharing. However, the time-shared approach reduces the achievable data throughput and also requires a challenging synchronization between the data packets of the different standards.

Due to the limitations of present coexistence solutions and the increasing number of standards in handheld devices, there is an interest to find alternative solutions to the coexistence problem. In addition, transmitter leakage in FDD systems [3] faces a similar problem as coexistence in multi-standard devices.

To avoid desensitization in the above situations, a high dynamic range has to be implemented in the receiver, leading to high power consumption. However, because of the limited energy resources available in handheld devices, minimizing the power consumption is critical. Thus, a major challenge will be to achieve low power consumption with a high dynamic range.

This paper proposes an RF amplifier that enables a frequency-independent suppression of a 0 to +11 dBm blocker by >35 dB while consuming 7–35 mW. Thanks to this suppression, the dynamic-range requirements for the subsequent stages in the receiver are relaxed. The suppression is achieved by an adaptive nonlinear circuit: the nonlinear transfer function creates the ability to provide different gains for signals having different amplitude levels [4]. By continuously adapting the circuit's nonlinear function according to the blocker amplitude, the gain of the blocker is effectively minimized while the gain of the signal remains high. Since the method requires knowledge of the amplitude of the interferer, it is most suitable for tackling the interference due to RX/TX or FDD coupling.

14.2 Principle of Operation

Nonlinear transfer functions exhibit properties that are fundamentally different from linear transfer functions, and thereby they enable different solutions in coexistence scenarios. This is illustrated in Fig. 14.1, where the input and output signals in both frequency and time domain for various conditions are compared. When passing a strong sinusoidal signal through a conventional compressive nonlinear system, the signal gets distorted and as a result harmonics are created (Fig. 14.1b). Here only odd order harmonics result because of the point-symmetric shape of the transfer function, a situation encountered in differential circuits. Considering the special case of the third order polynomial input/output relationship as shown in Fig. 14.1c, it appears that there even exist specific situations for which only a third order harmonic is generated, and the fundamental component is completely removed. The calculations describing this effect are stated below:

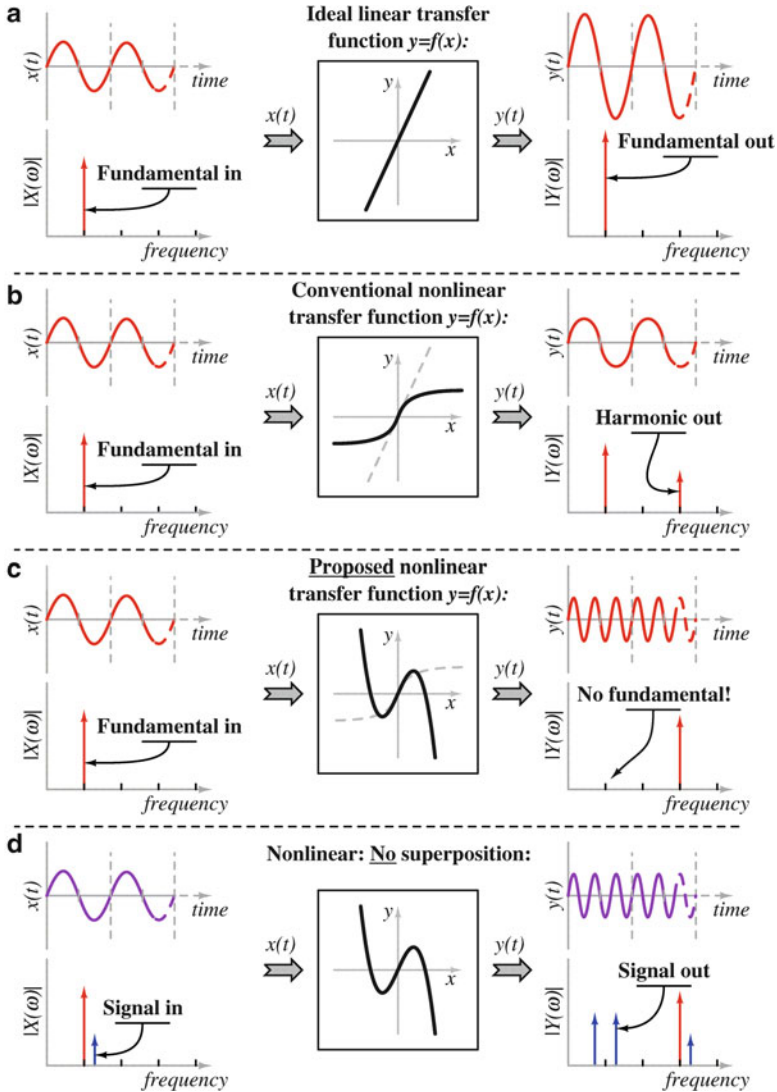


Fig. 14.1 (a) Ideally, circuits in radio receivers possess a linear transfer function. (b) In common practice however, receiver circuits generally have a nonlinear transfer function, leading to compression of the fundamental and the generation of harmonics.(c) Specifically tailored nonlinear transfers have the ability to fully suppress the fundamental for a specific input amplitude level. (d) Furthermore, weak (desired) signals, superimposed on the strong signal, are not suppressed and can even be amplified

$$\begin{aligned}
 y(t) &= x(t) + c_3 x^3(t) \\
 x(t) &= A_{LS} \sin(\omega_{LS} t) \\
 y(t) &= \left[A_{LS} + c_3 \frac{3A_{LS}^3}{4} \right] \sin(\omega_{LS} t) + c_3 \frac{A_{LS}^3}{4} \sin(3\omega_{LS} t)
 \end{aligned}$$

By choosing the third order coefficient c_3 equal to:

$$c_3 = -\frac{4}{3A_{LS}^3}$$

the output $y(t)$ becomes:

$$\rightarrow y(t) = \frac{A_{LS}}{3} \sin(3\omega_{LS} t)$$

Moreover, because nonlinear transfer functions do not obey the principle of superposition, a (much weaker) signal accompanying the strong signal undergoes a different operation. Excitation of the same nonlinear transfer function by the sum of the strong sinusoid with a weak sinusoid is shown in Fig. 14.1d. In contrast to the fundamental of the strong signal, the fundamental of the weak signal is not removed, but is still on its original location in the spectrum.

Next to the effect on the fundamental components of both large and small signals, the nonlinear operation also generates harmonics and intermodulation (IM) products. The harmonics can be removed easily by filtering at RF and because f_{LS} and f_{SS} are different, their IM products can be removed after down-conversion by filtering in the baseband. Of interest are the large- and small-signal gains, which in the rest of this paper are defined as the ratio between their fundamental output and fundamental input.

14.2.1 Strong-Signal Suppression Using a Zigzag Transfer Function

Achieving the functionality discussed in the previous section can be achieved with a wide variety of nonlinear transfer functions. Next to the example of the third order polynomial, the nonlinear transfer function shown in Fig. 14.2a (zigzag function) also achieves strong-signal suppression. The general requirements on the nonlinear transfer functions are discussed in more detail in [5]. Generally, it can be stated that the transfer must possess at least three zero-transitions, a property that is indeed seen in both the third order polynomial as well as the zigzag transfer. The zigzag transfer can be realized by combining the outputs of a linear amplifier and a clipping amplifier, and is therefore more suited considering the practicality of the concept. To demonstrate the concept using the zigzag transfer, the input spectrum consists of a strong and a weak

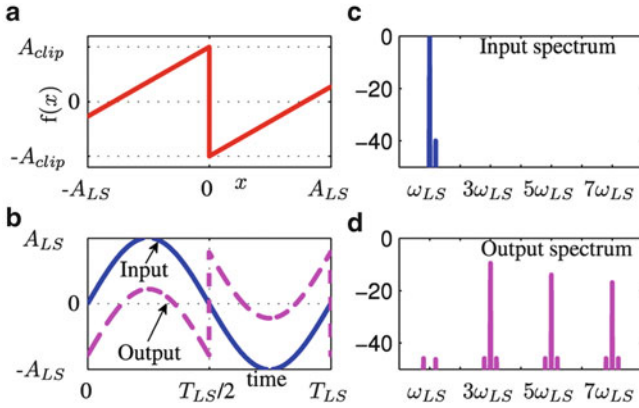


Fig. 14.2 (a) Zigzag transfer function. (b) Input (solid blue) and output (dashed magenta) signal versus time for a slope of unity for $[-A_{LS}, 0)$ and $(0, A_{LS}]$ in (a). (c) Input spectrum (blue) and (d) output spectrum (magenta) in dB relative to the input signal strength, illustrating the elimination of the fundamental

tone (Fig. 14.2c). This leads to an output spectrum consisting of several harmonics, but the fundamental of the strong signal is eliminated (Fig. 14.2d). To achieve this, the clipper amplitude A_{clip} must be set to:

$$A_{clip} = \frac{\pi}{4} A_{LS} G_{lin} \tag{14.1}$$

where A_{LS} is the amplitude of the strong signal (i.e. interferer) at the input and G_{lin} is the gain of the linear amplifier. As becomes clear from Eq. 14.1, A_{clip} must be adjusted according to A_{LS} to assure zero strong-signal gain. So, successful application of this principle requires the circuitry to adapt its transfer function to the instantaneous strong-signal amplitude level (Fig. 14.2a). Furthermore, the gain of the weak signal is equal to $G_{lin}/2$ [5]. So, by assuring at least 6 dB of gain in the linear amplifier, the weak signal is amplified whereas the blocker is eliminated.

14.2.2 Application to Multi-radio Transceivers

In case two standards A and B are simultaneously active in a multi-radio transceiver, a situation is encountered where the receiver of standard A (victim) is plagued by the strong transmitted signal of standard B (aggressor). The blocking signal injected into the victim receiver is known, because the signal of the aggressor is generated in the same device. Therefore, it is possible to determine the amplitude level of the aggressor as it appears at the NIS input. This knowledge is required for proper operation, as clarified in the previous sections. In Fig. 14.3b a sub-block “Magnitude” is analyzing the baseband signal the aggressor is transmitting, resulting in the determination of the actual strong-signal amplitude A_{LS} . A sub-block “NIS control”

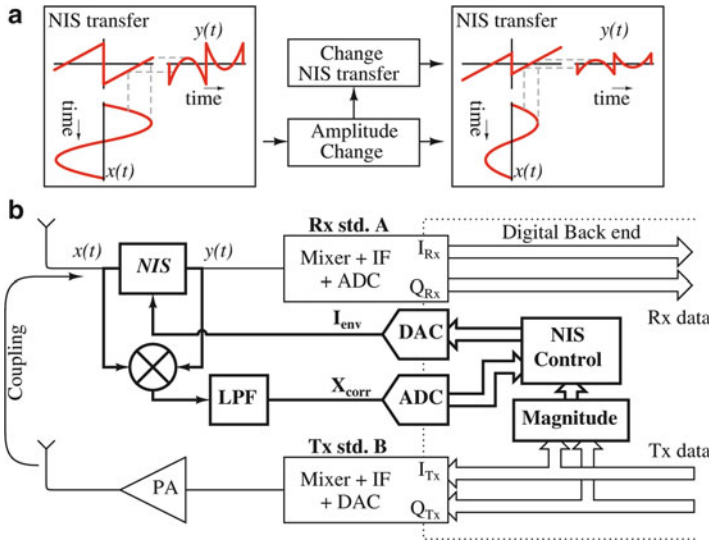


Fig. 14.3 (a) NIS input–output transfer adaptation for a change in input amplitude. (b) System level application of the NIS principle

on its turn steers the nonlinear interference suppressor (NIS) with a control current I_{env} using feed-forward, creating the desired blocker suppression.

Next to the feed-forward path, a mixer is present that multiplies the input with the output of the NIS. This operation results in the cross-correlation between these signals. The minimization of the cross-correlation means maximization of the suppression of the aggressor’s signal (assuming the aggressor’s signal to be dominant). The output of the mixer is being fed back into the “NIS control”, and thereby it provides a measure for the residual error in the control current I_{env} . Errors in I_{env} could be caused by e.g. changes of the coupling between the aggressor and the victim. This procedure is described in more detail in [6], and will in future be extended to cases with varying envelopes. The remainder of this document will concentrate on the implementation and performance of the analog hardware that is mandatory for the NIS concept, namely the NIS circuit with the mixer followed by the low-pass filter.

14.3 Circuit Implementation in CMOS

Figure 14.4 shows the NIS circuit diagram. Firstly, transistors M_1 – M_4 make up a linear amplifier resulting in a linear input–output relationship. Secondly, M_5 – M_8 make up a clipper circuit with adjustable output clipping amplitude. The desired zigzag transfer function is realized by combining the outputs of these two sub-circuits with the required polarity.

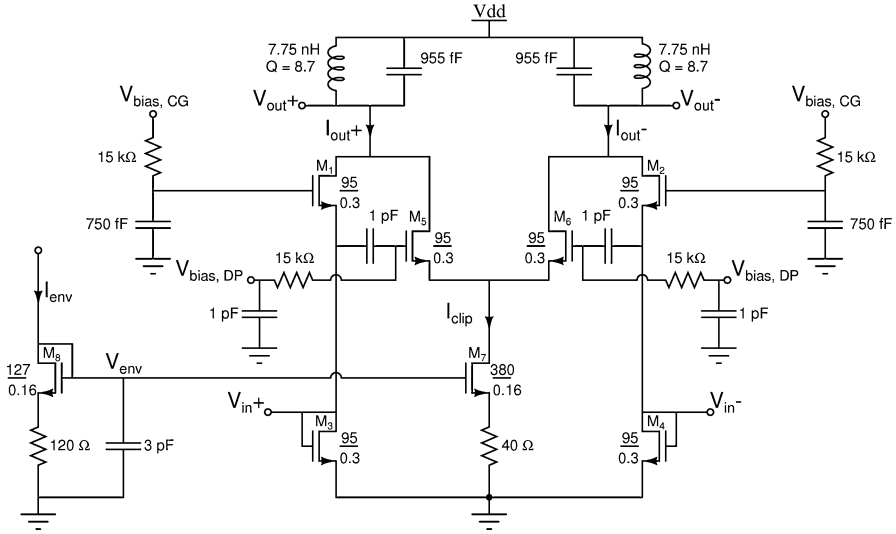


Fig. 14.4 NIS circuit diagram

$V_{bias,CG}$ is chosen such that M_1 – M_4 are just conducting, resulting in a class-AB bias. In case of a large signal being present at the input, either M_1 and M_4 , or M_2 and M_3 conduct causing the input resistance to be fairly constant around 60Ω . For small and large (rail-to-rail) input signals the input return is therefore approximately -12 dB. Because the output current of the transconductor is about half the input current, the transconductance is therefore quite linear.

Next, current I_{clip} is steered through either the left or right LC tank because transistors M_5 and M_6 act as switches (clipper circuit). These transistors are configured in common-source, causing the M_5 – M_6 structure to behave with opposite polarity with respect to the M_1 – M_4 structure, which is configured in common-gate. By combining the output currents of both parts, the desired zigzag transfer function is created.

External control over I_{clip} is provided through current mirror M_7 – M_8 . By adjusting I_{env} , the adaptivity of the transfer shape is thereby provided. As Fig. 14.2 shows, the NIS concept generates several higher order harmonics. To suppress these harmonics, the circuit is loaded with an LC tank. The LC tank assures high impedance around the fundamental frequency, while it shorts the higher harmonics. In case I_{clip} is set in accordance to Eq. 14.1, the strong-signal is suppressed, and the circuit behaves in NIS mode. If there is no need for strong signal suppression, I_{clip} must set to zero. In that case the clipper circuit is not activated, resulting in a classical amplifier response (only M_1 – M_4 are active).

A prototype IC, including ESD protection is implemented in $0.14\mu\text{m}$ CMOS [7]. The system on the chip includes the NIS circuit and the passive mixer with a single pole low-pass filter shown in Fig. 14.5. For measurement purposes, both the RF and LPF outputs are followed by buffer circuits. The chip photo of the prototype is shown in Fig. 14.6a. The chip has been packaged in a HVQFN24 package and

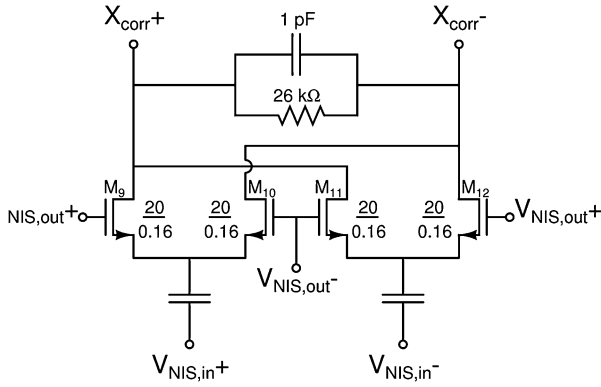


Fig. 14.5 Cross-correlation mixer circuit diagram

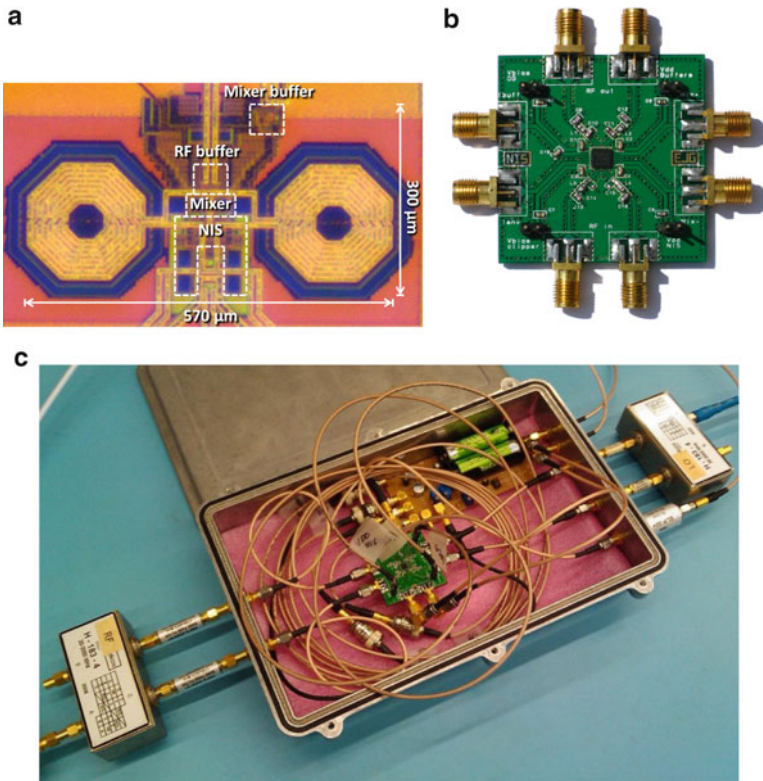


Fig. 14.6 Implemented NIS hardware. (a) Die photo. (b) PCB with packaged NIS chip (44 × 44 mm). (c) NIS PCB in Faraday cage including battery-based power supply/biasing

mounted on an FR4 PCB shown in Fig. 14.6b. Lastly, the PCB has been placed into an aluminum box making up a Faraday cage to guarantee full control over the signals applied to the system.

14.4 Experimental Results

The measured circuit transfer is maximal at 1.85GHz with a 3 dB bandwidth of 210 MHz. In both amplifier and NIS mode S_{11} is below -12 dB and S_{22} is below -13 dB. In this section first the characteristics in NIS mode, and then in amplifier mode are discussed.

14.4.1 NIS Mode

First, to demonstrate the NIS operation, a measurement is conducted by exciting the chip by the combination of a strong signal (0 dBm) and weak signal (-59 dBm). Both signals are phase modulated, and the spacing of the carrier frequency is limited to only 2 MHz. Because of the phase modulation, the envelope of the blocker is constant causing the spectral content of I_{env} to consist of only a DC signal. I_{env} is optimized such that the blocker gain is minimized. The input signal and output signal of this measurement after optimizing I_{env} are shown in Fig. 14.7.

As can be seen, the ratio between the blocker and the signal has been reduced by almost 50 dB. Next to the suppression of the blocker, also an additional tone has been created. This additional tone is an intermodulation product between the desired signal and the blocker. In general, it can be stated that the output of a memory-less nonlinear function around the fundamental when excited with a strong and a weak sinusoidal signal is equal to [8]:

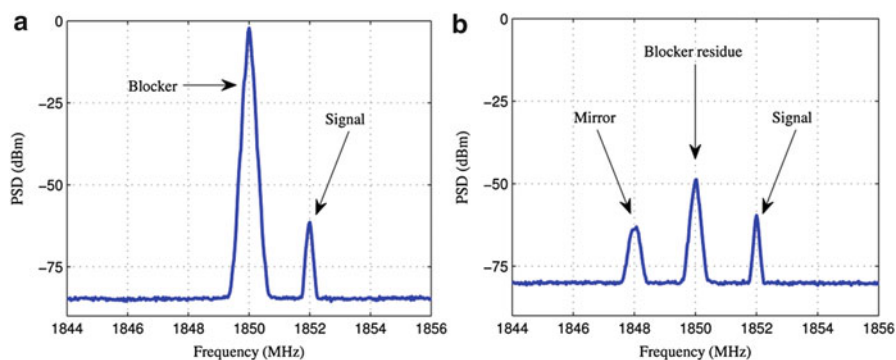


Fig. 14.7 Measured NIS response. (a) Input spectrum. (b) Output spectrum

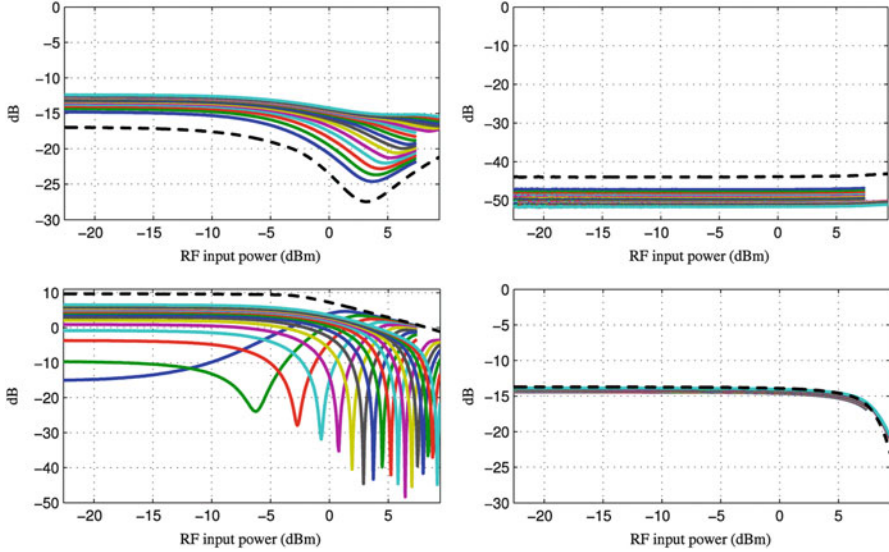


Fig. 14.8 Measured large-signal S-parameters for $I_{env} = 0.4\text{--}3.8$ mA with steps of 0.2 mA. The response for $I_{env} = 0$ mA is shown with the *black dashed lines*. (a) S_{11} . (b) S_{12} . (c) S_{21} . (d) S_{22}

$$y(t) = G_{LS} \cdot Int(t) + \frac{1}{2} \left[A_{LS} \cdot \frac{\delta G_{LS}}{\delta A_{LS}} + G_{LS} \right] \cdot s(t) \quad (14.2)$$

$$+ \frac{1}{2} \left[A_{LS} \cdot \frac{\delta G_{LS}}{\delta A_{LS}} - G_{LS} \right] \cdot IM(t)$$

The signals in the above equations are given by:

$$Int(t) = A_{LS} \cdot \sin[\omega_{LS}t + \varphi_{LS}]$$

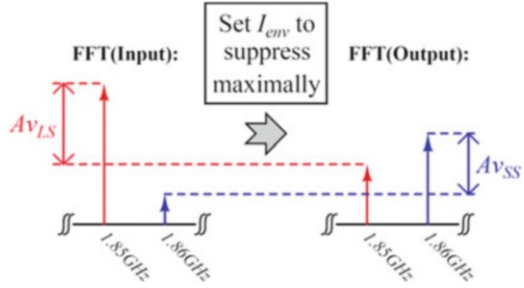
$$s(t) = A_{LS} \cdot \sin[\omega_{LS}t + \varphi_{LS}]$$

$$IM(t) = A_{SS} \cdot \sin[(2\omega_{LS} - \omega_{SS})t + 2\varphi_{LS} - \varphi_{SS}]$$

Here, G_{LS} is the gain of the strong signal, $\omega_{SS} = 2\pi f_{SS}$ and $\omega_{LS} = 2\pi f_{LS}$. From Eq. 14.2 it can be concluded that in case of strong-signals suppression (i.e. $G_{LS} = 0$), the magnitude of the content at ω_{SS} and $(2\omega_{LS} - \omega_{SS})$ in $y(t)$ are equal. This conclusion is in agreement with the measurement results shown in Fig. 14.7 (although the power spectral density of the mirrored component is less than that of the signal, their powers are equal).

Next, the large-signal S-parameters are measured of the NIS chip for different values of I_{env} . The results of this measurement are shown in Fig. 14.8. The transfer-controlling

Fig. 14.9 Graphical representation in the frequency domain of the strong- and weak-signal gain measurement procedure



current I_{env} has been varied from 0.4 mA to 3.8 mA in steps of 0.2 mA, and the circuit is excited by a single tone at 1.85GHz, whose amplitude has been swept from -22 up to 9.5 dBm. As a reference, the response in case of $I_{env} = 0$ has been added as well, which is identified as amplifier mode. S_{21} in amplifier mode shows a 1dB of about -4 dBm as can be seen. Beyond that, the NIS operation becomes feasible. As can be concluded from the figure, S_{11} , S_{22} and S_{12} show a small variation compared to the variation observed in S_{21} , and provide sufficient performance (i.e. input and output reflection below -12 dB and reverse isolation below -40 dB). The response of S_{21} illustrates the amplitude domain filtering property that is aimed for in the NIS concept. By choosing a specific value for I_{env} , the zigzag transfer is configured such that a specific amplitude level is suppressed, according to Eq. 14.1.

Measuring both the gain for the strong blocker and the gain for the weak signal is conducted using the approach illustrated in Fig. 14.9. The input is excited by the sum of a weak signal and a strong signal. Then, the output is analyzed and I_{env} is chosen such that the strong signal is minimized. This procedure has been automated by closing the loop shown in Fig. 14.3b using an FPGA based PXI of National Instruments with AD/DA interface.

The measurement results from this procedure are shown in Fig. 14.10, for different values of $V_{bias,CG}$ in Fig. 14.4. Figure 14.10a shows the voltage gain of the strong signal, and Fig. 14.10b shows the voltage gain of the weak signal. The ratio between these two gains is identified as the strong signal suppression, which is shown in Fig. 14.10c. Although theory predicts that no cross-modulation takes place between the strong blocker and the weak signal in case of an ideal clipper/amplifier combination [5], it is seen in Fig. 14.10b that this is not fully achieved. This discrepancy is caused by the non-ideal behavior of mainly the clipper, i.e. the gain of the clipper during zero-transitions is dependent on the value of I_{env} , which on its turn depends on the amplitude of the strong signal. By lowering $V_{bias,CG}$, the dynamic range over which Av_{SS} varies, reduces.

Another observation that can be done is that although Av_{LS} is low, it never reaches zero. The cause of the limitation on the amount of suppression lies in the presence of memory effects. Memory effects in the circuit cause a phase mismatch between the linear amplifier and the clipper, causing imperfect cancellation. The ideal phase difference between the two sub-circuits of 180° is therefore not perfectly achieved. The choice of $V_{bias,CG}$ is identified here as a trade-off between

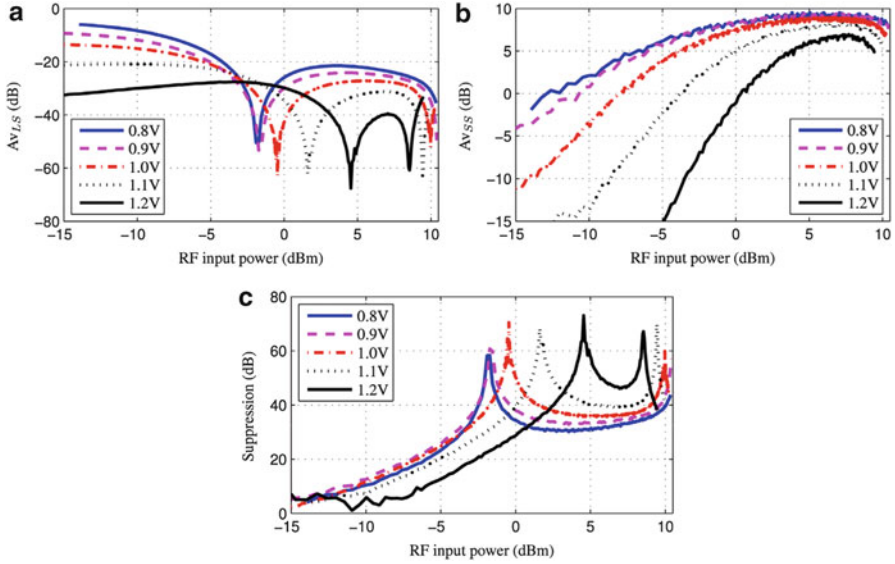


Fig. 14.10 Measured NIS behavior for different values of $V_{bias,CG}$. (a) Strong signal voltage gain. (b) Weak signal voltage gain. (c) Strong signal suppression

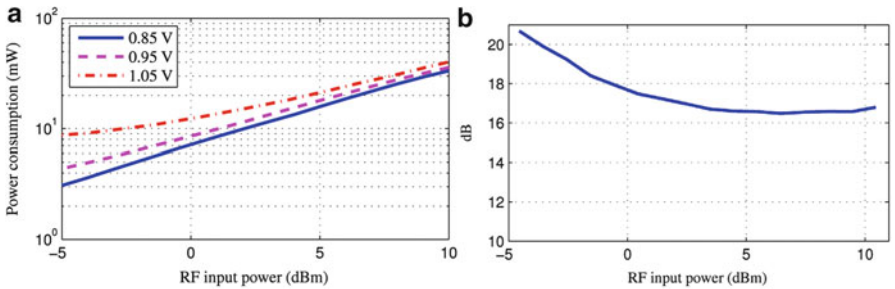


Fig. 14.11 NIS power consumption and noise figure. (a) NIS P_{DC} for different values of $V_{bias,CG}$. (b) Noise figure ($V_{bias,CG} = 1V$)

on the one hand weak signal gain (magnitude and flatness) and dynamic range, versus on the other hand the amount of suppression the circuit achieves. The power consumption and the noise figure of the NIS circuit versus the input level of the suppressed RF signal (i.e., blocker) are shown in respectively Fig. 14.11a, b.

The power consumption decreases with decreasing RF input power because of the class AB operation of the circuit, governing the absolute value of the power consumption to be low as well. The measured noise figure is just above 16 dB. As can be seen in the circuit diagram of Fig. 14.4, the input is connected to MOS

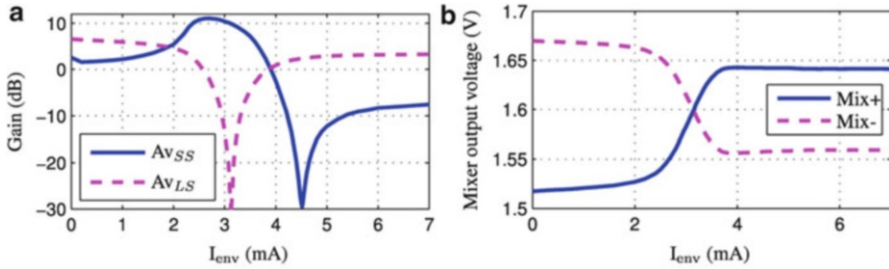


Fig. 14.12 Verification of the behavior of the cross-correlation mixer. (a) Weak & strong signal gain versus I_{env} . (b) Mixer output versus I_{env}

diodes that do not contribute to the gain of the circuit, but do dissipate the RF signal, which is not beneficial for the noise performance. Besides this effect, another aspect that complicates low noise design is the combination of an input–output path made up of M_1 – M_2 configured in common gate and an input–output path made up of M_5 – M_6 configured in common source. Both paths have different optimal source impedances regarding noise performance, so a trade-off occurs. Lastly, because of the spectrum mirroring effect discussed in the beginning of this section and derived using (2), the noise of $(2\omega_{LS}-\omega_{SS})$ folds into the frequency band of the desired signal, causing a minimal noise figure inherent to the NIS concept of 3 dB.

Next, the behavior of the mixer that is present on the IC is evaluated. To illustrate the behavior of the mixer, a measurement is performed by measuring its differential output voltage while increasing I_{env} , and maintaining the same input signal. The RF input of the NIS circuit is excited with a sinusoidal tone of 8 dBm during this measurement. The results are shown in Fig. 14.12, with the voltage gain of the weak and strong signal in Fig. 14.12a and the mixer output in Fig. 14.12b. As can be seen, the mixer outputs become equal in case the strong signal is minimized, indicating proper operation.

14.4.2 Amplifier Mode

By setting current I_{clip} to zero (shorting V_{env} to ground), the chip is set to amplifier mode. Characterization of the IC was done here by measuring the gain, noise figure and IIP3. In Fig. 14.13a the simulated as well as the measured voltage gain can be seen versus $V_{bias,CG}$. As the figure shows, the measured performance is worse than the simulated performance. This reduced performance is mainly explained by a lower than expected transconductance of the transistors, and a lower quality factor of the LC tank. The noise performance is shown in Fig. 14.13b. Also with respect to noise performance a reduction is seen from simulation to measurement. The IIP₃ of the chip was measured to be 6.6 dBm for a $V_{bias,CG}$ of 1.15 V.

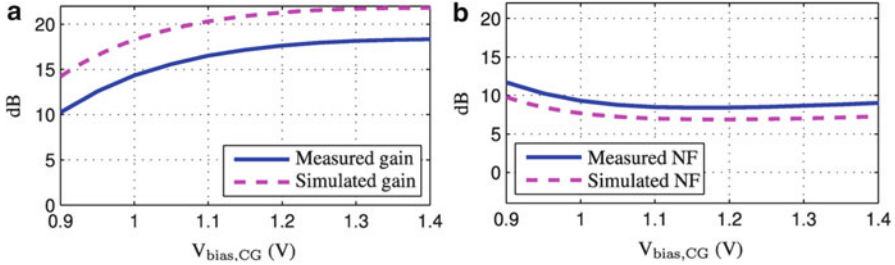


Fig. 14.13 Behavior of the chip in amplifier mode. (a) Voltage gain. (b) Noise figure

14.5 Summary and Conclusions

A 1.8 GHz RF amplifier implemented in 0.14 μm CMOS with frequency-independent blocker suppression has been presented. The blocker suppression functionality is obtained by continuously adapting the nonlinear transfer function of the circuit according to the blocker amplitude. Application areas are coexistence scenarios where the envelope of the blocker to be suppressed is known, for example in multi-radio devices and standards dealing with TX leakage in FDD systems.

The circuit has two modes of operation: the NIS mode, when it provides blocker suppression, and the amplifier mode, when no blocker is present at the input. In NIS mode, a voltage gain for weak signals of respectively 7.6–9.4 dB and $\text{IIP3} > 4\text{dBm}$ were measured in the presence of a 0 to +11 dBm RF blocker, while the blocker has been suppressed by more than 35 dB. Analysis predicted, and measurements confirmed that in case of blocker suppression using the proposed NIS method signals and noise are mirrored to the image frequency with respect to the blocker. A passive mixer has been put on the chip to derive the cross-correlation between input and output with the aim of determining the amount of blocker suppression achieved. The mixer has been used in a feedback loop, and showed the expected behavior. The noise figure in NIS mode has been measured to be just above 16 dB. The reason for this relatively high value is partly due to the specific circuit topology, and partly is inherent to the NIS concept. Future research will concentrate on optimizing the circuit topology and finding measures to counteract the spectrum mirroring taking place when using the concept.

The circuit is set to amplifier mode in case there is no blocker present at the input. In amplifier mode, the circuit provides 17 dB of voltage gain and an IIP3 of 6.6 dBm while consuming 3 mW. The performance in measurements has dropped with respect to the simulations because of a reduction in transistor transconductance and quality factor of the LC tank. The 1 dB compression point of the circuit is found to be about -4dBm , which is around the same value where the NIS concept becomes feasible. So, for interferers of up to -4dBm the circuit can be operated in amplifier mode, whereas for higher interferer levels, the NIS mode should be used.

References

1. S. Sheng, RF coexistence – Challenges and opportunities, in *Radio Frequency Integrated Circuits Symposium (RFIC) IEEE*, Baltimore, USA, 5–7 June 2011
2. J. Zhu, A. Waltho, X. Yang, X. Guo, Multi-radio coexistence: Challenges and opportunities, in *Computer Communications and Networks. ICCCN. Proceedings of 16th International Conference on*, Honolulu, USA, 13–16 Aug 2007, pp. 358–364
3. E.A. Keehr, A. Hajimiri, A rail-to-rail input receiver employing successive regeneration and adaptive cancellation of intermodulation products, in *Radio Frequency Integrated Circuits Symp. (RFIC) IEEE*, Anaheim, USA, 23–25 May 2010
4. K.J. Friederichs, A novel canceller for strong CW and angle modulated interferers in spread-spectrum-receivers, in *Military Communications Conference MILCOM. IEEE*, Los Angeles, USA, vol. 3, 21–24 Oct 1984, pp. 478–481
5. E.J.G. Janssen, H. Habibi, D. Milosevic, P.G.M. Baltus, A.H.M van Roermund, Frequency-independent smart interference suppression for multi-standard transceivers, in *IEEE European Microwave Conference (EuMC)*, Amsterdam, Oct 28th – Nov 2nd 2012
6. H. Habibi, E.J.G. Janssen, W. Yan, J.W.M. Bergmans, P.G.M. Baltus, Suppression of constant modulus interference in multimode transceivers by closed-loop tuning of a nonlinear circuit, in *Vehicular Technology Conference (VTC Spring), 2012 IEEE*, Yokohama, Japan, 6–9 May 2012
7. E.J.G. Janssen, D. Milosevic, P.G.M. Baltus, A 1.8GHz amplifier with 39dB frequency-independent smart blocker suppression, in *IEEE Radio Frequency Integrated Circuits Symposium (RFIC)*, Montreal, June 2012
8. N. Blachman, Band-pass nonlinearities. *IEEE Trans Inf Theory* **10**, 162–164 (1964)